Polymer Testing 34 (2014) 34–41

Contents lists available at ScienceDirect

Polymer Testing

journal homepage: www.elsevier.com/locate/polytest

Test method

Torsion test method for mechanical characterization of PLDLA 70/30 ACL interference screws

C.R.M. Roesler [a], G.V. Salmoria [a,b], A.D.O. Moré [a], J.M. Vassoler [c], E.A. Fancello [a,c,*]

[a] Laboratório de Engenharia Biomecânica (LEBm), Hospital Universitário, Universidade Federal de Santa Catarina, 88040-900 Florianópolis, SC, Brasil
[b] Laboratório CIMJECT, Departamento de Engenharia Mecânica, Universidade Federal de Santa Catarina, 88040-900 Florianópolis, SC, Brasil
[c] GRANTE, Departamento de Engenharia Mecânica, Universidade Federal de Santa Catarina, 88040-900 Florianópolis, SC, Brasil

ARTICLE INFO

Article history:
Received 24 October 2013
Accepted 6 December 2013

Keywords:
Torsion test
Bioabsorbable screws
PLDLA

ABSTRACT

This study developed a test method for determining the mechanical properties of poly-L/D-lactide (PLDLA) 70/30 cannulated bioabsorbable anterior cruciate ligament (ACL) interference screws. We proposed a method that defines three characteristic lengths associated with the screw void space, which was designed to receive the screwdriver during insertion of the implant: (1) the clamping length Lc, (2) the screwdriver insertion length Lb, and (3) the gauge length Lg. We tested twenty completely fabricated and finished screws that had been submitted to different levels of hydrolytic degradation. In torsion tests, the variables measured were stiffness, yield torque, yield torque angle, maximum torque and maximum torque angle. These values were correlated with the fracture surface, numerical simulation and molecular weight. The results of the degradation testing, lasting from 0 to 240 days, show a clear transition in the screws' mechanical behavior from ductile to brittle. We concluded that the proposed torsion testing method is appropriate for determining the mechanical properties of cannulated polymeric screws.

1. Introduction

Bioabsorbable implants manufactured by injection molding are widely used in orthopedic surgery, and their worldwide market is expanding rapidly [1,2]. One of their most popular uses is as interference screws in reconstructive knee surgery for a ruptured anterior cruciate ligament (ACL) (Fig. 1).

Absorbable screws have some advantages relative to metallic ones, including the absorption of the implant once its function has ceased, the absence of magnetic resonance imaging (MRI) artifacts, and a decrease in graft lacerations [3]. Furthermore, reports indicate that there is no difference in fixation strength between absorbable and metallic screws [4,5].

The mechanical demands on the implant may be divided into two distinct stages. During surgical insertion, the screw is submitted mainly to torsional and axial loads, while lateral compression and longitudinal shear forces are applied during clinical use [6]. It has been reported, however, that absorbable screws are more likely to break during surgery [7–11]. For this reason, an assessment of the mechanical behavior of the screws for this loading condition is necessary.

The technical standard ASTM F2502 (*Standard Specification and Test Methods for Bioabsorbable Plates and Screws for Internal Fixation Implants)* provides a standard test

* Corresponding author. Departamento de Engenharia Mecânica, Universidade Federal de Santa, Catarina, 88040-900 Florianópolis, SC, Brasil.
E-mail addresses: fancello@grante.ufsc.br, efancello@gmail.com (E.A. Fancello).

0142-9418/$ – see front matter © 2013 Elsevier Ltd. All rights reserved.
http://dx.doi.org/10.1016/j.polymertesting.2013.12.005

method for measuring the mechanical properties of polymer crews in torsion. According to this standard, "the fully threaded screw is placed in the holding device so that five threads, below the head of the screw, are exposed outside the holding device. A large enough portion of the screw thread should be gripped to firmly secure the screw so that it does not rotate when under torsional load". The torque is applied by inserting the screwdriver (bit) into the screw head. However, unlike solid core osteosynthesis screws, cannulated interference bioabsorbable screws have a cylindrical orifice along almost their entire length to the screwdriver connection.

Weiler [12] and Costi [13] conducted studies in which cannulated screws were embedded in resin, simulating their being jammed into the bone tunnel. With a fully inserted screwdriver, increasing torque was applied up to the point of screw breakage. Despite these attempts to replicate the clinical procedure for fixing the screws and their medical relevance, this method cannot test the mechanical properties of the screw, since the fully inserted screwdriver does not induce adequate torsional effort on the device.

The objective of this study is to develop an appropriate method for testing cannulated polymeric screws under torsion and to characterize a specific set of mechanical properties. Considering that bioabsorbable implants are designed to gradually reduce in mechanical strength and mass during degradation [14–16], we applied our proposed method in a degradation study of poly-L/D-lactide (PLDLA) 70/30 screws in order to capture the changes of mechanical properties of these screws during degradation.

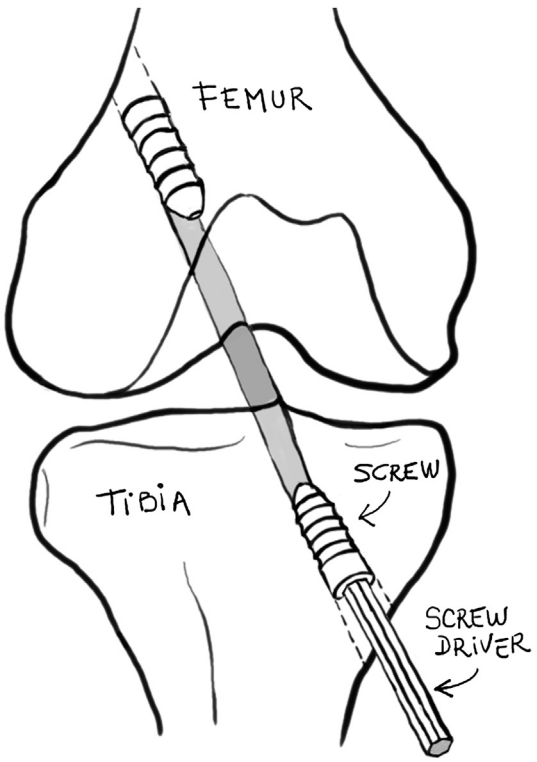

Fig. 1. Interference screws in reconstructive surgery of the ACL.

2. Experimental setup

Twenty 6 mm × 20 mm fabricated and finished interference bioabsorbable PLDLA 70/30 screws, supplied by MDT Implantes®, Rio Claro, SP – Brazil (Fig. 2), were used. Five of them were tested in the initial (virgin) condition, while the other fifteen (5 + 5 + 5) were tested after 60, 120 and 240 days of degradation.

Screws submitted to degradation were placed in buffered saline solution at physiologic temperature (37 °C), and samples were periodically removed for testing. For each time period, the samples were analyzed using gel permeability chromatography (GPC) to measure their corresponding molecular weight [g/mol], according to ASTM F1635 (*Standard Test Method for in vitro Degradation Testing of Hydrolytically Degradable Polymer Resins and Fabricated Forms for Surgical Implants*). Measurements were performed on a Viscotek model VE 2001 GPC system equipped with four p-Styragel columns with exclusion limits of 10^6, 10^5, 10^4 and 10^3 angstroms, respectively. Operating conditions included the solvent THF, the solute PLA and polystyrenes, an injected volume of 200 microlitres, a sample concentration of 0.1 wt %, a column temperature of 45 °C and a flow rate of 1 mL/min. The polystyrenes were injected as a mixture of three or four narrow fractions.

For the torsion test, each screw sample was vacuum-dried 24 h after removal from the degradation solution and then fixed on the specimen holder using a cold-hardening adhesive resin. To measure the mechanical properties of the polymeric screw under torsion, three characteristic screw lengths were defined: the gauge length (Lg) = 7.0 mm, the clamping length (Lc) = 7.2 mm and the screwdriver insertion length (Lb) = 5.8 mm (see Fig. 2). The purpose of defining an insertion length smaller than the full insertion length is to force the screw to break in a region not occupied by the metallic screwdriver, therefore being submitted to torsion efforts.

The screw was placed within the specimen holder using an alignment device consisting of an external cylinder and a centering cone (Fig. 3). The tip of screw was fixed along the Lc using 0.2 g of cold hardening adhesive resin (3M Scotch-Weld DP-460). The system was kept within the alignment device for 96 hours to ensure the complete cure of the resin.

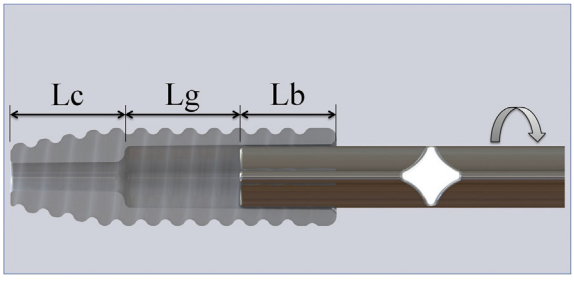

Fig. 2. Characteristic lengths defined for testing: clamping length (Lc), gauge length (Lg) and screwdriver insertion length (Lb).

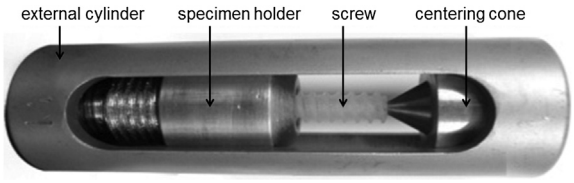

Fig. 3. Alignment device.

The torsion tests were performed on a torsion test machine INSTRON model 55 MT at 23 °C and 38% RH. The specimen holder with the screw was mounted in the torsion testing machine. The screwdriver was then inserted into the screw along length *Lb* and axial rotation was applied at a constant rate of 1 rpm. A torque load cell with a linearity range from 0.09 to 22.5 Nm at +/−0.5% accuracy was used. The torque vs. angular displacement was recorded at a rate of 500 Hz. The measured variables during torsion testing were stiffness [Nmm/deg], yield torque [Nm], yield torque angle [deg], maximum torque [Nm] and maximum torque angle [deg].

After each test, the specimens were submitted to fractographic analysis using a scanning electron microscope (SEM) to investigate the failure surface appearance. The samples were then mounted on aluminum stubs with adhesive carbon tape and coated with a thin layer of gold using a sputter coater (D2 Diode Sputtering System). Microscopy was performed using a Jeol JSM-6390LV operating at an accelerating voltage of 15 kV.

Additionally, the experimental setup was reproduced virtually and analyzed using the Finite Element Method to gain deeper insight into the strain and stress distributions occurring in such a complex geometry during the test.

3. Results and discussion

3.1. Torsion testing curves

The curves of torque versus angle of rotation obtained with the virgin screws are shown in Fig. 4.

All these curves show an initial (visco) elastic quasi-linear region that lasts up to the so-called torsional yield angle. Beyond this angle, permanent (visco) plastic strain occur, a phenomenon that is reflected in this case by a clear change in the slope of the torque-angle curves. As long as the rotation proceeds, strain localization takes place, as does damaging of the polymeric structure, leading to microvoids, coalescence, fracture propagation and ultimate failure of the device. In Fig. 4, one can see that after 100 degrees of rotation there is a significant dispersion of the unloading (failure) curves. As already mentioned, this last unloading is related to progressive slippage and breakage (failure) of the polymeric chains.

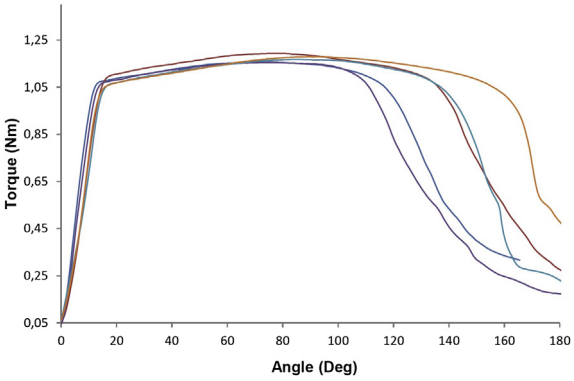

Fig. 4. Torque versus angle of rotation curve for virgin screws.

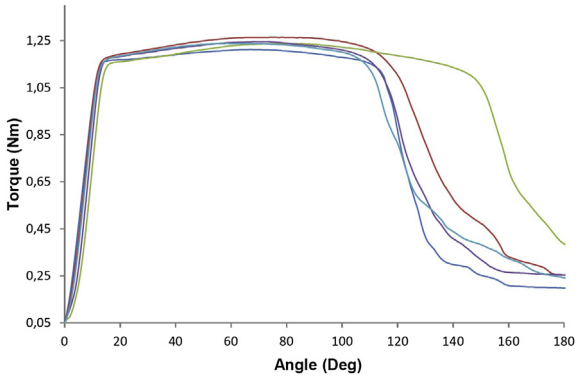

Fig. 5. Torque versus angle of rotation curve for screws after 60 days of degradation.

Figs. 5 and 6 show the curves of torque versus angle of rotation obtained after 60 and 120 days of degradation, where it is possible to see the reduction in the average failure angle for both cases, especially for the screws with 120 days of degradation.

For all curves in Figs. 5 and 6, again we identify the (visco) elastic stage followed by the (visco) plastic stage and the final loss of mechanical integrity. It is well known that elongation in mechanical tests decreases with the decrement of molecular weight. This is a critical phenomenon in the progression of hydrolysis and its effects on torsion behavior. From a clinical point of view, the paired torque–angle of yielding is relevant, since it is related to clinical failure during screw implantation. From the material perspective, maximum torque and failure angle are

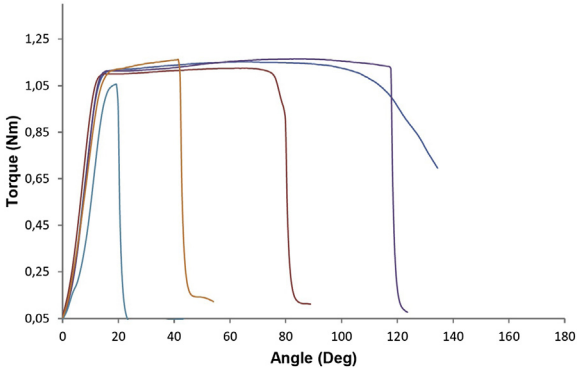

Fig. 6. Torque versus angle of rotation curve for screws after 120 days of degradation.

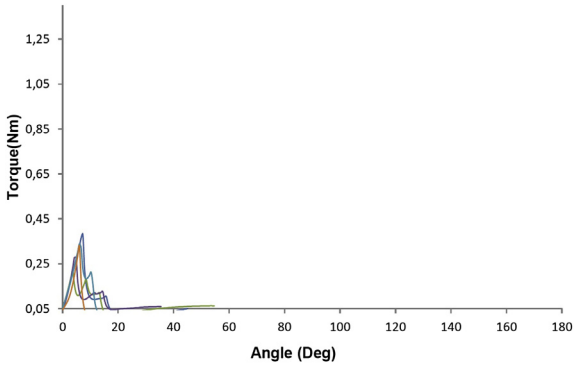

Fig. 7. Torque versus angle of rotation curve for screws after 240 days of degradation.

relevant for characterizing the material resistance and degradation behavior. Fig. 7 shows the torsion behavior of screws after 240 days of degradation, where it is evident that the plastic region disappears, resulting in purely brittle behavior. Since it is no longer possible to define a yield torque, strong reductions in the maximum torque and in the torsional stiffness can be quantified.

Table 1 summarizes the values of the main torsional properties of the PLDLA screws. The average values of stiffness were 70.0 Nmm/deg for virgin (time zero, T0) screws. The average values for screws with 60, 120 and 240 days degradation were 80.9, 72.5 and 54.0 Nmm/deg, respectively. These values show a slight variation during the first 120 days followed by a clear decrement at 240 days due to polymeric chain length reduction caused by hydrolysis. A similar tendency is observed in the average values of the yield strength. While small variations are seen up to 60 days (1073–1156 Nmm), a significant decrement occurs beyond 120 days (725 Nmm). As already pointed out, sometime between 120 and 240 days the plastic region disappears and the yield torque transforms to maximum torque, with an average of 349 Nmm. Finally, the average failure angle decreases continuously from time zero to 240 days.

To summarize the whole process, we can say that the first modified property is the failure angle (related to the material toughness and ductility), followed by the yield torque (related to the material yield strength), and finally the torsional stiffness (related to the Young's modulus of the material). This behavior is consistent with the concept that polymeric chains shorten during degradation.

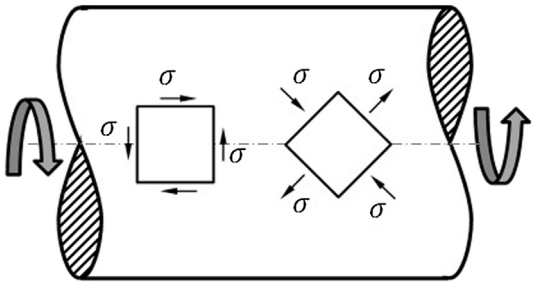

Fig. 8. Stress state of a circular cylinder under torsion.

3.2. Fractography results

To better analyze the fractography results, we recall the stress state in a solid or hollow cylindrical sample subjected to torsion, as represented in Fig. 8.

Planes perpendicular and parallel to the sample axis are submitted to pure shear stresses while planes oriented 45° to this axis are submitted to maximum normal tensile and normal compressive stresses with magnitudes equal to those of the shear stresses. This stress distribution, together with the material's mechanical properties, determines the characteristics of the fracture surface in these devices. A brittle material will not withstand high tensile stresses and fracture propagation will happen in a plane at a 45° angle to the cylinder axis, forming a helicoidal fracture surface. On the other extreme, a compliant material allows the planes under shear stress to slide along each other, inducing plastic shear strains that, after localization, resulting in ductile fracture propagation.

Despite the fact that the geometry of the screws analyzed in this study is far from being a regular cylinder with annular section, the above discussion still applies and the two extreme cases of fracture mentioned above were found in the torsion tests of the virgin screws and in screws after 240 days of degradation.

Fig. 9 shows micrographs at different magnifications of the fractured surface of a virgin screw (T0). The top left slide of the entire transversal section (fractured plane) shows a very rough surface with clear radial lines and cavitation marks that suggest the final stage of a plastic deformation process (chain slippage) in the transversal twisting planes.

In contrast to the T0 (virgin) screws, screws tested after 240 days of degradation seem to have failed in a brittle

Table 1
Torsional properties and molecular weight of PLDLA screws.

Specimen	Stiffness [Nmm/deg] ± SD	Yield torque [Nmm] ± SD	Yield angle [deg] ± SD	Max torque [Nmm] ± SD	Max torque angle [deg] ± SD	Failure angle ± SD	Molecular weight Mw (g/mol)
Condition1 (time zero)	70.0 ± 6.0	1073 ± 17	16.70 ± 1.30	1168 ± 16	85.42 ± 6.29	133.47 ± 20.09	90,704 ± 11,410
Condition2 (60 days)	80.9 ± 5.6	1156 ± 25	15.86 ± 0.68	1144 ± 237	67.34 ± 25.30	120.26 ± 16.01	91,018 ± 2865
Condition3 (120 days)	72.5 ± 9.0	725 ± 9	16.51 ± 1.88	1123 ± 46	49.44 ± 26.07	73.56 ± 43.17	67,588 ± 2179
Condition4 (240 days)	54.0 ± 13.0	–	–	349 ± 112	8.28 ± 1.38	5.45 ± 1.48	38,235 ± 7869

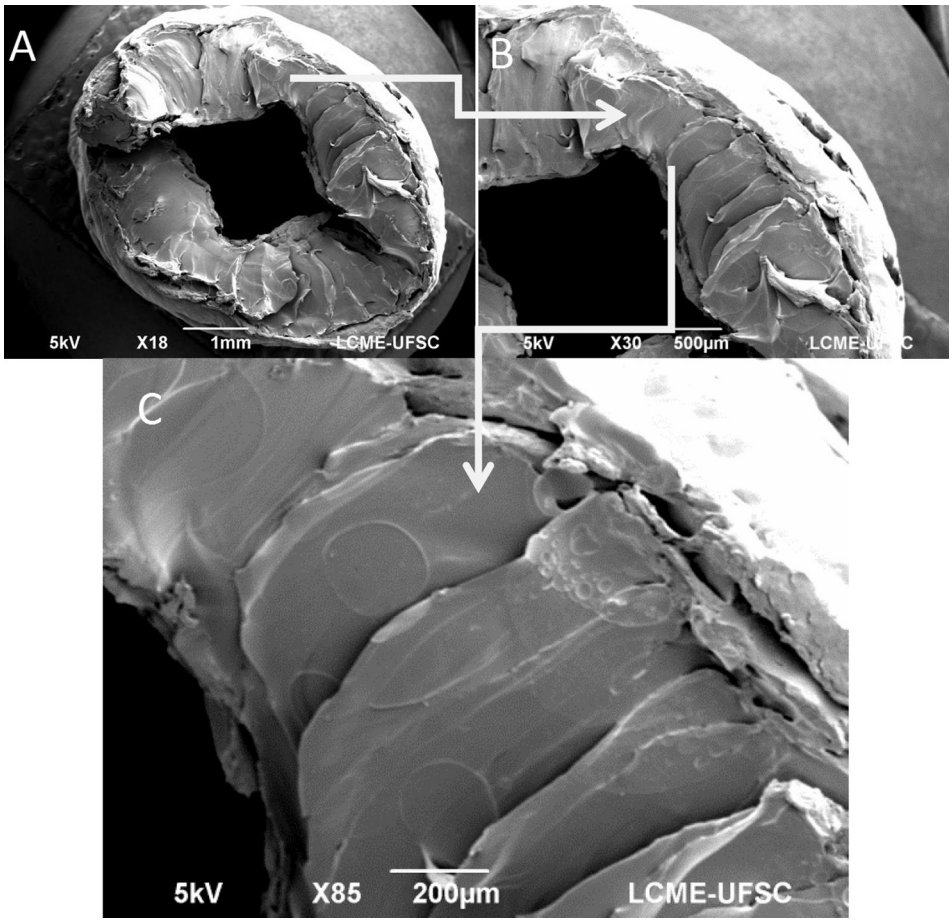

Fig. 9. Micrographs of a virgin screw T0 after torsion test: (A) SEM image of whole fractured transversal surface, (B) detail at 30 times magnification, and (C) detail at 85 times magnification.

manner. Fig. 10(A) shows the fractured surface near the head of the screw in a view parallel to the cylinder axis. Fig. 10(B) shows the characteristic features of a fast and brittle failure, with the fracture origin area near the internal surface of the screw, surrounded by radial marks typically found in high-speed flaw failure propagation [18]. The fracture in these specimens runs helicoidally. The origin of the fracture is near the second thread valley from the screw head, which is consistent with the highest principal tensile stress observed in the simulation at 5 degrees of rotation (Section 3.3, Fig. 14).

These results, i.e., ductile versus brittle fracture, molecular weight reduction and reduction of failure angle in torsion curves at different times of degradation seem to show some consistent correlations. When the polymeric screw maintains its long chains and molecular integrity, failure can be expected at the end of an accumulated plastic strain in localized regions and, consequently, is ductile in appearance. Conversely, when the material's molecular chains shorten due to degradation during hydrolysis, its failure mechanism changes gradually from ductile to fragile as it becomes much more susceptible to tensile stresses.

3.3. Numerical simulation

To gain deeper insight into the distribution of the strains and stresses occurring in the screw's complex geometry during the test, we reproduced the experimental setup virtually and analyzed it using the finite element method. To this aim, we generated a mesh of tetrahedral elements within the 3D geometry of the screw, using plane elements to define the rigid surface of the screwdriver. The representation of this mesh is shown in Fig. 11.

The surface of the screw tip was clamped while a controlled rotation was prescribed for the screwdriver, reproducing the same boundary conditions as those of the experiment. Appropriate unilateral (contact) conditions were set between the surface of the screwdriver and the inner surface of the screw. To model the mechanical response of the PLDLA screw, an elasto-plastic constitutive model (no hardening) was used (according to the von Mises yield function and Prandtl–Reuss flow rule [17]). This simple constitutive model is controlled by material parameters such as the Young's modulus E, Poisson Coefficient ν and Yield limit σ_y. The values were identified by inverse analysis to minimize the difference between

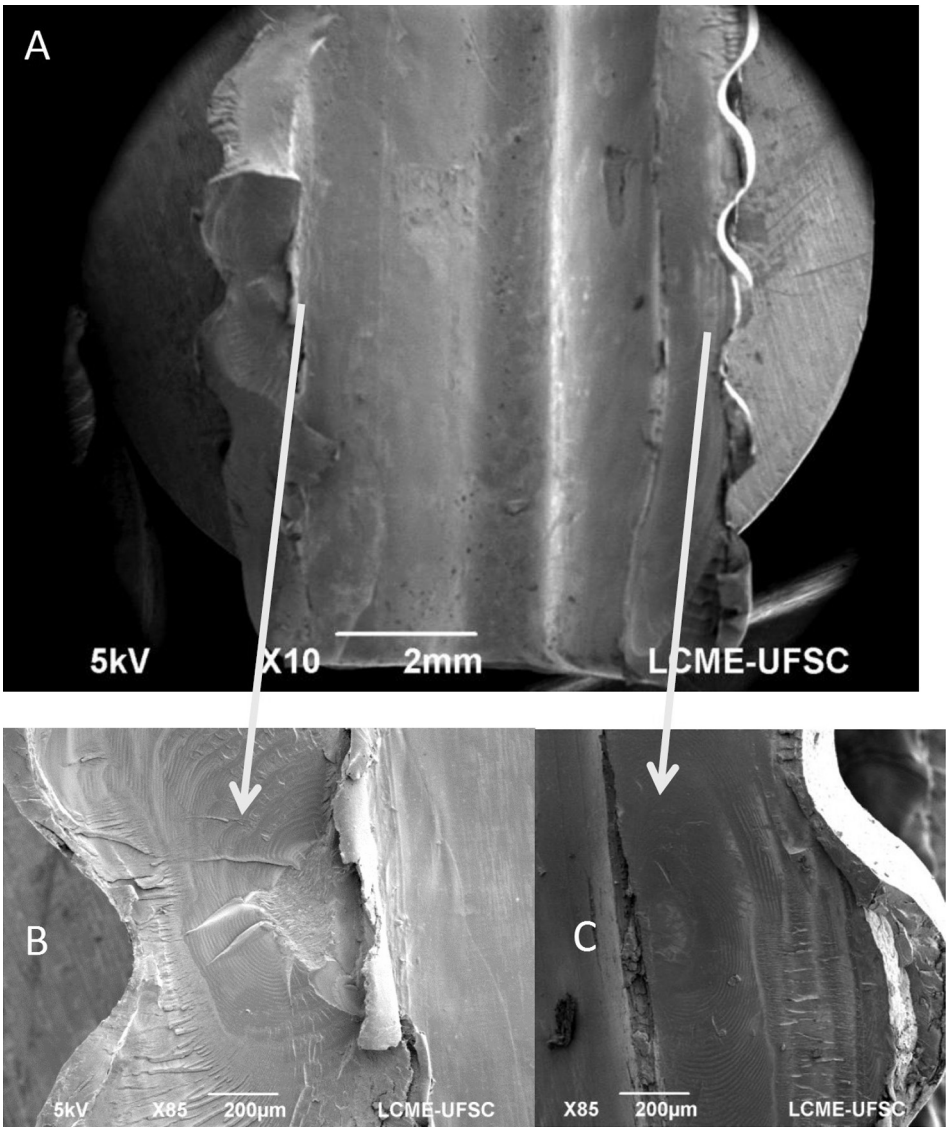

Fig. 10. Micrographs of virgin screw after torsion test: (A) SEM image of lateral view, (B) SEM of one fracture origin at 30 times magnification, and (C) second fracture origin image at 85 times magnification.

numerical and experimental torque versus the rotation curves. The obtained values were $E = 1.800$ MPa, $\nu = 0.2$, and $\sigma_y = 67$ MPa. Fig. 12 shows both the experimental and numerical curves.

Fig. 13 shows the distribution of equivalent accumulated plastic (permanent) strains that occur at 30 degrees of screwdriver rotation. Again, maximum values are found near the head of the screw, just below the screwdriver tip, which correlates with the position of the transversal fracture surface in the virgin screws (see Fig. 9). Fig. 14 shows the distribution of the maximum principal stress over the screw at 5 degrees of rotation, which is the approximate angle when fracture occurs. It is evident that the highest stress concentrations occur near the fracture origin observed in Fig. 10 on the degraded specimen.

Although a more sophisticated material model is needed to better represent the complex behavior of thermoplastic polymers such as PLDLA, the correlation between the experimental and numerical curves in this case is acceptable. The correlation provides a clearer picture of the plastic strain distribution along the screw, making it possible to identify the region where fracture initiation is most probable. This correlation also reinforces the advantages of using appropriate simulations for design purposes.

4. Conclusions

We have proposed a new method for testing cannulated polymeric screws under torsion. The method was applied to PLDLA 70/30 screws used in surgery for reconstructing the ACL of the human knee. According to our results, this

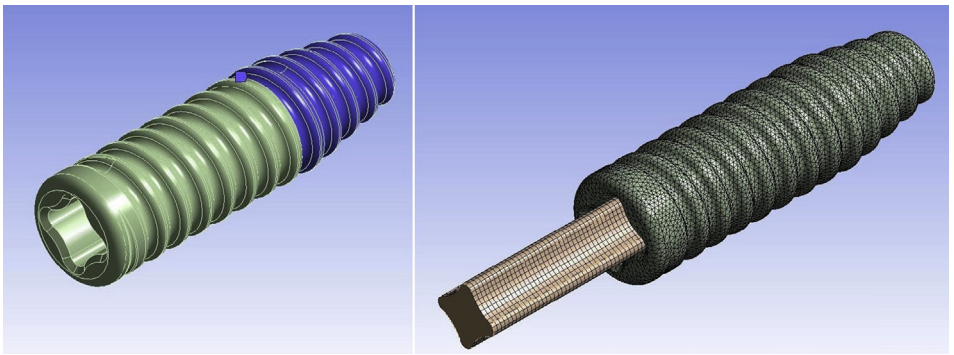

Fig. 11. Images of screw geometry and finite elements mesh for the screw and screwdriver.

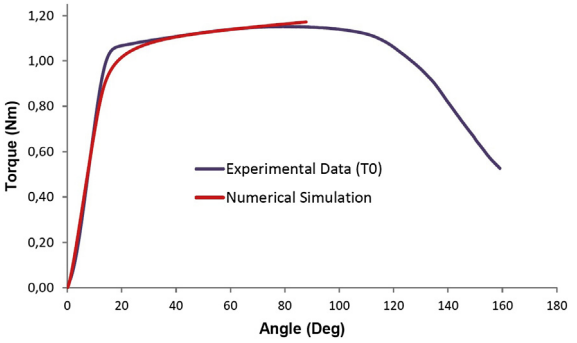

Fig. 12. Experimental average and numerical torque versus rotation curves.

method was able to capture a set of mechanical properties of the polymeric screws and to identify significant differences in these properties when the screws are exposed to hydrolysis. The variables measured included stiffness, yield torque, yield torque angle, maximum torque and maximum torque angle. All these values were captured from the torsion curves. The results show a clear transition of the screws' mechanical behavior from ductile to fragile as the degradation time increases from zero to 240 days. Fracture surfaces of virgin screws show ductile behavior with radial lines and cavitation marks, suggesting a final stage of a plastic deformation process (chain slippage) in the transversal twisting planes. In contrast, degraded screws present typical brittle fracture surfaces at the origin, and a mirror smooth area and rough hackle periphery due to decreasing crack propagation velocity.

The average stiffness value was 70.0 Nmm/deg for virgin (T0) screws while the average values for screws after 60, 120, and 240 days degradation were 80.9, 72.5 and 54.0 Nmm/deg, respectively. These values show a slight variation during the first 120 days followed by a clear decrement at 240 days due to reduction in the polymeric chain length caused by the hydrolysis. A similar tendency was observed in the average values of the yield strength. While small variations are seen up to 60 days

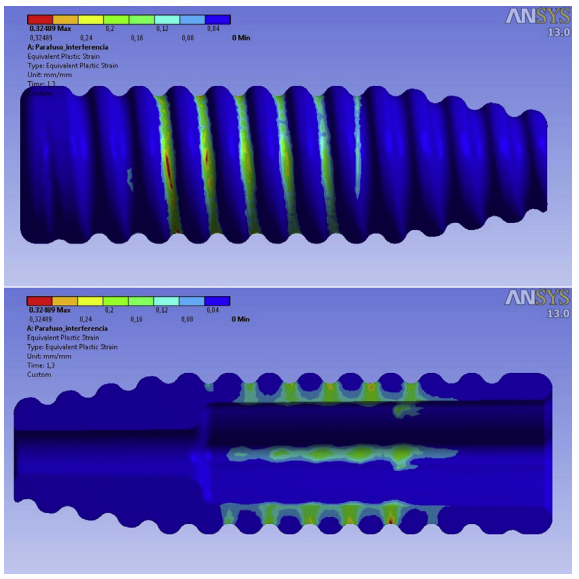

Fig. 13. Equivalent accumulated plastic strains achieved at 30° of rotation (displayed on the undeformed screw configuration).

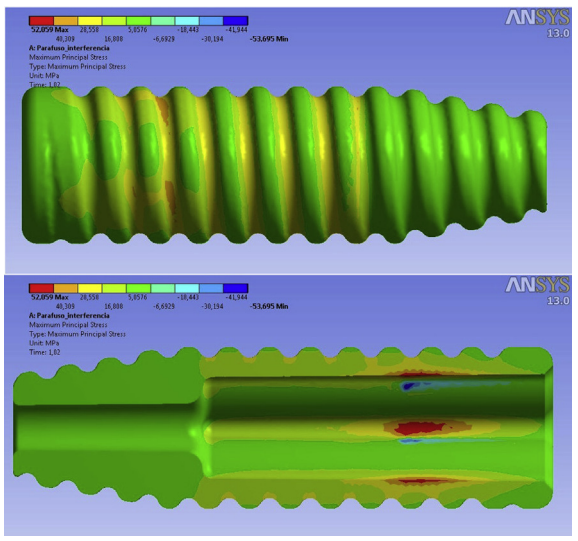

Fig. 14. Maximum principal stress achieved at 5° of rotation (displayed on the undeformed screw configuration).

(1073–1156 Nmm), a significant decrement is observed beyond 120 days (725 Nmm). Sometime between 120 and 240 days, the plastic region disappears and the yield torque transforms to maximum torque, with an average of 349 Nmm.

To gain deeper insight into the strain and stress distribution occurring in the screw's complex geometry during the test, the experimental setup was reproduced virtually and analyzed using the finite element method. Numerical analysis of the stress distribution agrees with the experimental results for the PLDLA screws.

On the basis of all these results, we can conclude that the proposed torsion test is suitable for determining the mechanical properties of cannulated polymeric screws.

Acknowledgements

The authors would like to thank PRONEX-FAPESC, FINEP, CNPq, and CAPES for their financial support.

References

[1] S. Konan, F.S. Haddad, A clinical review of bioabsorbable interference screws and their adverse effects in anterior cruciate ligament reconstruction surgery, Knee 16 (1) (2009) 6.
[2] C.G. Ambrose, T.O. Clanton, Bioabsorbable implants: review of clinical experience in orthopedic surgery, Ann. Biomed. Eng. 32 (1) (2004) 171.
[3] F. Alan Barber, B.F. Elrod, D.A. McGuire, L.E. Paulos, Bioscrew fixation of patellar tendon autografts, Biomaterials 21 (24) (2000) 2623.
[4] A. Almazan, A. Miguel, A. Odor, J.C. Ibarra, Intraoperative incidents and complications in primary arthroscopic anterior cruciate ligament reconstruction, Arthroscopy 22 (11) (2006) 1211.
[5] D. Andersson, K. Samuelsson, J. Karlsson, Treatment of anterior cruciate ligament injuries with special reference to surgical technique and rehabilitation: an assessment of randomized controlled trial, Arthroscopy 25 (6) (2009) 653.
[6] S.A. Rodeo, S.P. Arnoczky, P.A. Torzilli, C. Hidaka, R.F. Warren, Tendon-healing in a bone tunnel. A biomechanical and histological study in the dog, J. Bone Joint Surg. Am. 75 (12) (1993) 1795.
[7] D.J. Beevers, Metal vs bioabsorbable interference screws: initial fixation, Proc. Inst. Mech. Eng. H 217 (1) (2003) 59.
[8] P. Kousa, T.L. Jarvinen, P. Kannus, M. Jarvinen, Initial fixation strength of bioabsorbable and titanium interference screws in anterior cruciate ligament reconstruction. Biomechanical evaluation by single cycle and cyclic loading, Am. J. Sports Med. 29 (4) (2001) 420.
[9] A. Kotani, Y. Ishii, Reconstruction of the anterior cruciate ligament using poly-L-lactide interference screws or titanium screws: a comparative study, Knee 8 (4) (2001) 311.
[10] D.A. McGuire, F.A. Barber, B.F. Elrod, L.E. Paulos, Bioabsorbable interference screws for graft fixation in anterior cruciate ligament reconstruction, Arthroscopy 15 (5) (1999) 463.
[11] F.A. Barber, B.F. Elrod, D.A. McGuire, L.E. Paulos, Preliminary results of an absorbable interference screw, Arthroscopy 11 (5) (1995) 537.
[12] A. Weiller, H.J. Windhagen, M.J. Raschke, A. Laumeyer, R.F.G. Hoffmann, Biodegradable interference screw fixation exhibits pull-out Force and stiffness similar to titanium screws, Am. J. Sports Med. 26 (1) (1998) 119.
[13] J.J. Costi, A.J. Kelly, T.C. Hearn, D.K. Martin, Comparison of torsional strengths of bioabsorbable screws for anterior cruciate ligament reconstruction, Am. J. Sports Med. 29 (5) (2001) 575.
[14] G. Lajtai, G. Schmiedhuber, F. Unger, G. Aitzetmüller, M. Klein, I. Noszian, E. Orthner, Bone tunnel remodeling at the site of biodegradable interference screws used for anterior cruciate ligament reconstruction: 5-year follow-up, Arthroscopy 17 (6) (2001) 597.
[15] O. Kilicoglu, M. Demirhan, S. Akman, A.C. Atalar, S. Ozsoy, U. Ince, Failure strength of bioabsorbable interference screws: effects of in vivo degradation for 12 weeks, Knee Surg. Sport Traumatol. Arthrosc. 11 (4) (2003) 228.
[16] A. Weiler, R. Peine, A. Pashmineh-Azar, C. Abel, N.P. Sükamp, R.F.G. Hoffmann, Tendon healing in a bone tunnel. Part 1: biomechanical results after biodegradable interference fit fixation in a model of anterior cruciate ligament re- construction in sheep, Arthroscopy 18 (2) (2002) 113.
[17] E. de Souza Neto, D. Peric, D.R.J. Owens, Computational Methods for Plasticity: Theory and Applications, John Wiley & Sons Ltd., 2008.
[18] T. Tan, F. Ren, J.J.A. Wang, E. Lara-Curzio, P. Agastra, J. Mandell, W.D. Bertelsen, C.M. LaFrance, Investigating fracture behavior of polymer and polymeric composite materials using spiral notch torsion test, Engineering Fracture Mechanics 101 (2013) 109.